Microbiology

Porphyromonas gingivalis methionine gamma lyase is one of the hydrogen sulfide productive enzymes from L-cysteine and enhances mouse abscess formation

--Manuscript Draft--

Manuscript Number:	MIC-D-17-00420R1
Full Title:	Porphyromonas gingivalis methionine gamma lyase is one of the hydrogen sulfide productive enzymes from L-cysteine and enhances mouse abscess formation
Article Type:	Research Article
Section/Category:	Host-microbe interaction
Corresponding Author:	Akihiro Yoshida, Ph.D., D.D.S. Matsumoto Dental University Shiojiri, JAPAN
First Author:	Suguru Nakamura
Order of Authors:	Suguru Nakamura
	Koki Shioya
	B. Yukihiro Hiraoka
	Nao Suzuki
	Tomonori Hoshino
	Taku Fujiwara
	Nobuo Yoshinari
	Toshihiro Ansai
	Akihiro Yoshida, Ph.D., D.D.S.
Abstract:	Porphyromonas gingivalis produces hydrogen sulfide (H2S) from L-cysteine. However, the role of H2S produced by P. gingivalis in periodontal inflammation is unclear. In this study, we identified the enzyme that catalyzes H2S production from L-cysteine, and analyzed the role of H2S using a mouse abscess model. The identified enzyme was identical to methionine-gamma-lyase (PG0343), which produces methyl mercaptan (CH3SH) from L-methionine. Therefore, we analyzed H2S and CH3SH production by P. gingivalis W83 and a PG0343-deletion mutant (PG0343) with/without L-cysteine and/or DL-methionine. The results indicated that CH3SH is produced constitutively irrespective of the presence of L-methionine, while H2S is greatly increased by both P. gingivalis W83 and PG0343 in the presence of L-cysteine. In contrast, CH3SH production by PG0343 was absent irrespective of the presence of L-methionine, and H2S production was eliminated in the absence of L-cysteine. Thus, CH3SH and H2S production involves different substrates, L-methionine or L-cysteine, respectively. Based on these characteristics, we analyzed the roles of CH3SH and H2S in abscess formation in mice by P. gingivalis W83 and PG0343. Abscess formation by P. gingivalis W83, but not PG0343, differed significantly in the presence and absence of L-cysteine. In addition, the presence of L-methionine did not affect the size of abscesses generated by P. gingivalis W83 and PG0343. Therefore, we conclude that H2S produced by P. gingivalis does not induce inflammation; however, H2S enhances inflammation caused by CH3SH. Thus, these results suggest the H2S produced by P. gingivalis plays a supportive role in inflammation caused by methionine-gamma-lyase.

Powered by Editorial Manager® and ProduXion Manager® from Aries Systems Corporation

Manuscript Including References (Word document)

Click here to download Manuscript Including References (Word document) Pg Microbiology 180108R1.docx

Revised 1. (MIC-D-17000420)

Porphyromonas gingivalis methionine gamma lyase is one of the hydrogen sulfide productive enzymes from L-cysteine and enhances mouse abscess formation

Suguru Nakamura[1, 2], Koki Shioya[3], B. Yukihiro Hiraoka[4], Nao Suzuki[5], Tomonori Hoshino[6], Taku Fujiwara[7], Nobuo Yoshinari[1], Toshihiro Ansai[2], Akihiro Yoshida[3*]

[1]Department of Periodontology, Matsumoto Dental University, Shiojiri, Japan
[2]Division of Community Oral Health Science, Department of Oral Health Promotion, Kyushu Dental University, Kitakyushu, Japan
[3]Department of Oral Microbiology, Matsumoto Dental University, Shiojiri, Japan
[4]Institute of Oral Science, Matsumoto Dental University, Shiojiri, Japan
[5]Department of Preventive and Public Health Dentistry, Fukuoka Dental College, Fukuoka, Japan
[6]Department of Pediatric Dentistry, School of Dentistry, Meikai University, Saitama, Japan.
[7]Department of Pediatric Dentistry, Nagasaki University Graduate School of Biomedical Sciences, Nagasaki, Japan.

Address of institution at which the work was performed: Department of Oral Microbiology, Matsumoto Dental University, Shiojiri, 390-0781, Japan
Tel & Fax: +81-263-51-2082

*correspondence: Akihiro Yoshida, [redacted]
Tel. and Fax.: +81-263-51-2082

Short title: Effect of hydrogen sulfide of *Porphyromonas gingivalis* on mouse abscess formation

Keywords: *Porphyromonas gingivalis*, hydrogen sulfide, L-cysteine, abscess

Subject category: Host-Microbe Interaction

Abbreviations: ANOVA, analysis of variance; BHI, brain heart infusion; CBB, Coomassie Brilliant Blue; GAM, Gifu Anaerobic Medium; HOMD, Human Oral Microbiome Database; LPS, lipopolysaccharide; NTA, nitrilotriacetic acid; TLCK, N^{α}-tosyl-L-lysinylchloromethane; TLR, Toll-like receptor; VSC, Volatile sulfur compound;

Abstract

Porphyromonas gingivalis produces hydrogen sulfide (H_2S) from L-cysteine. However, the role of H_2S produced by *P. gingivalis* in periodontal inflammation is unclear. In this study, we identified the enzyme that catalyzes H_2S production from L-cysteine, and analyzed the role of H_2S using a mouse abscess model. The identified enzyme was identical to methionine-γ-lyase (PG0343), which produces methyl mercaptan (CH_3SH) from L-methionine. Therefore, we analyzed H_2S and CH_3SH production by *P. gingivalis* W83 and a PG0343-deletion mutant (ΔPG0343) with/without L-cysteine and/or DL-methionine. The results indicated that CH_3SH is produced constitutively irrespective of the presence of L-methionine, while H_2S is greatly increased by both *P. gingivalis* W83 and ΔPG0343 in the presence of L-cysteine. In contrast, CH_3SH production by ΔPG0343 was absent irrespective of the presence of L-methionine, and H_2S production was eliminated in the absence of L-cysteine. Thus, CH_3SH and H_2S production involves different substrates, L-methionine or L-cysteine, respectively. Based on these characteristics, we analyzed the roles of CH_3SH and H_2S in abscess formation in mice by *P. gingivalis* W83 and ΔPG0343. Abscess formation by *P. gingivalis* W83, but not ΔPG0343, differed significantly in the presence and absence of L-cysteine. In addition, the presence of L-methionine did not affect the size of abscesses generated by *P. gingivalis* W83 and ΔPG0343. Therefore, we conclude that H_2S produced by *P. gingivalis* does not induce inflammation; however, H_2S enhances inflammation caused by CH_3SH. Thus, these results suggest the H_2S produced by *P. gingivalis* plays a supportive role in inflammation caused by methionine-γ-lyase.

INTRODUCTION

Hydrogen sulfide (H_2S), a noxious gas, is, together with nitric oxide (NO) and carbon monoxide (CO), a signaling molecule in mammals [1]. H_2S has a variety of physiological functions, including neuromodulation, vasodilation, oxidant regulation, inflammation, and angiogenesis [2, 3]. H_2S freely diffuses through cell membranes to elicit various responses and modulate a variety of cellular events independently of membrane receptors or second messenger systems [4]. H_2S is produced endogenously via assimilatory sulfate reduction and cysteine degradation in both eukaryotes and prokaryotes [5]. The small amount of H_2S formed via the former mechanism is rapidly assimilated into organic sulfur compounds, such as sulfur-containing amino acids, and is not released extracellularly. In contrast, the latter mechanism—which involves cystathionine β-synthase (CBS), cystathionine γ-lyase (CSE), 3-mercaptpyruvate sulfurtransferase (3MST), and cysteine aminotransferase (CAT)—is responsible for large-scale H_2S generation [5]. In prokaryotes, H_2S confers resistance against antibiotics by stimulating reactive oxygen species (ROS) scavenging mechanisms [6, 7]. H_2S can scavenge ROS, thus preventing oxidative stress; however, it also has toxic properties [8]. Such diverse activities have led to conflicting data regarding the roles of H_2S in different organisms [9, 10].

Porphyromonas gingivalis is a Gram-negative obligatory anaerobe that causes chronic periodontal inflammation, which leads to alveolar bone resorption [11-15]. Recently, this bacterium is considered as "keystone-pathoegn" of the oral microbiota [16-18]. This bacterium enters the bloodstream, interacts with host organs and tissues, and ultimately contributes to the pathogenesis of cardiovascular disease and various systemic conditions [19-23]. *P. gingivalis* is known to produce volatile sulfer compounds (VSCs), such as H_2S, methyl mercaptan (methanethiol) and dimethyl sulfide, in serum [24, 25]. A previous study reported that *P. gingivalis* methionine-γ-lyase, which produces methyl mercaptan from L-methionine, is involved in murine abscess formation [26, 27]. In addition,

methyl mercaptan increases the permeability of subgingival porcine mucosa and induce interleukin-1β (IL-1β) secretion from mononuclear cells [28]. Thus, methyl mercaptan is considered as one of the major virulence factors of this organisms [29]. We reported previously that *P. gingivalis* produces H_2S by degrading cysteine [31]. H_2S derived from *P. gingivalis* upregulates IL-8 production by gingival and oral epithelial cells [32]. However, the role of H_2S in inflammatory periodontal disease is unclear.

In this study, we identified the *P. gingivalis* gene that encodes an enzyme that catalyzes H_2S production using L-cysteine as a substrate. Next, we evaluated the characteristics of the enzyme using gas chromatography. Finally, we assessed the role of *P. gingivalis* H_2S in inflammation using a *P. gingivalis* deletion mutant and performed a histological analysis of mice infected with *P. gingivalis*. The aim was to clarify the role of H_2S in inflammation caused by *P. gingivalis*.

METHODS

Bacterial strains and culture conditions

P. gingivalis W83 and its derivative strain were maintained anaerobically (10% CO_2, 10% H_2, 80% N_2) at 37°C in GAM broth (Nissui Medical Co., Tokyo, Japan) or brain heart infusion (BHI; Becton Dickinson, Sparks, MD) agar supplemented with hemin (5 μg/mL) and menadione (1 μg/mL). For antibiotic selection, cultures were supplemented with 10 μg/mL erythromycin.

Fractionation of *P. gingivalis* proteins

P. gingivalis culture medium was incubated with leupeptin and N^{α}-tosyl-L-lysinylchloromethane (TLCK; Sigma-Aldrich, St. Louis, MO), which are cysteine proteinases inhibitors, to prevent autoproteolysis. *P. gingivalis* cells from 400 mL of culture were resuspended in 8 mL of buffer A (20 mM Tris-HCl, pH 8.0), and disrupted by sonication at 150 W for 20 min (INSONATOR 201M; KUBOTA Corporation, Tokyo, Japan). After centrifugation (6,000 ×g for 15 min), the supernatant was

collected and dialyzed (Spectra/Por Dialysis Membrane, molecular weight cutoff, 6,000–8,000; Spectrum Laboratories) three times against 20 mM Tris-HCl, pH 8.0. The dialyzed medium was fractionated by gel filtration. For gel filtration, Sephacryl S-200 (GE Healthcare, Uppsala, Sweden) packed in a column (2.6 cm by 90 cm) was used. The column was eluted at a flow rate of 28 mL/h with 20 mM Tris-HCl buffer, pH 7.5 containing 150 mM NaCl.

H_2S assay

To isolate the enzyme involved in H_2S production from L-cysteine, enzymatic assays were performed as described previously, with minor modifications [31]. The protein fractions (fraction number 38 to 80) were suspended in a solution containing 200 mM triethanolamine-HCl (pH 8.0), 10 μM pyridoxal 5'-phosphate, 0.5 mM bismuth trichloride, 10 mM EDTA, 1% Triton X-100, and 20 mM L-cysteine. Enzymatic activities were measured at 37°C. The bismuth trichloride in the mixture reacted with sulfide to form a black precipitate (bismuth sulfide). H_2S production was confirmed by visually assessing precipitation of bismuth sulfide and measured at an optical density of 405 nm (OD_{405}). PG0343 activity was examined by measuring the rate of pyruvate formation as described previously [31]. Each 500 μL of reaction mixture contained 40 mM potassium phosphate buffer (pH 7.6), 5 nmol pyridoxal-5'-phosphate, 7.5 μg of the purified recombinant enzyme, and substrate at various concentrations. To determine pyruvate production, the reaction was terminated by adding 250μL of 4.5% trichloroacetic acid after incubation for 10 min at 37°C. The reaction mixture was centrifuged, and 250 μL of the supernatant were added to 750 μL of 0.33 M sodium acetate (pH 5.2) containing 0.017% 3-methyl-2-benzothiazolinone hydrazine. The reaction mixture was then incubated at 50°C for 30 min. The amount of pyruvate was determined by measuring the OD at 335 nm (OD_{335}) [33].

Identification of the enzyme-encoding gene

Protein fraction-formed bismuth sulfide precipitations were separated by native polyacrylamide gel electrophoresis (PAGE) and H_2S production was visualized according to Yoshimura *et al*. [34]. After

electrophoresis, the gel was incubated at 37°C in a solution containing 200 mM triethanolamine-HCl (pH 8.0), 10 μM pyridoxal 5'-phosphate, 0.5 mM bismuth trichloride, 10 mM EDTA, 1% Triton X-100, and 20 mM L-cysteine for H_2S production. The black precipitate formed in the presence of H_2S was excised from the gel, resolved by sodium dodecyl sulfate (SDS)-PAGE, and electrotransferred to a polyvinylidene difluoride (PVDF) membrane. The membrane was stained with 0.1% Coomassie Brilliant Blue (CBB) R-250 for 1 h, destained with 7.5% acetic acid containing 40% methanol, and washed with distilled water for 24 h. NH_2-terminal amino acid sequencing was performed by the Edman degradation method.

PAGE and immunoblotting

Bacterial proteins were resuspended in 5× Laemmli sample buffer or 5× Laemmli sample buffer without SDS, resolved by SDS-PAGE or native-PAGE, and electrotransferred to a PVDF membrane. The membrane was blocked with TBS containing 1% nonfat milk, incubated with a rabbit anti-*P. gingivalis* methionine-γ-lyase (PG0343) antibody, and subsequently incubated with a goat anti-rabbit IgG conjugated to alkaline phosphatase. Total protein was assayed to enable measurement of specific protein levels.

Generation of the *P. gingivalis* PG0343-deletion mutant

P. gingivalis PG0343 was identified in the Human Oral Microbiome Database (HOMD; The Forsyth Institute, http://www.homd.org/index.php). To delete *P. gingivalis PG0343*, the following plasmid was prepared. Two fragments, up- and down-stream of *PG0343*, were generated by PCR using the primers PG0343 UF-Apa/ PG0343 UR-Sph and PG0343 DF-Spe/PG0343 DR-Sac, respectively (Table 2). The products were digested using *Apa*I/*Sph*I and *Spe*I/*Sac*I, respectively, and ligated into pBluescript SKII$^+$, resulting in pPG0343UD (Table 1). To generate erythromycin resistance, an *ermF-ermAM* cassette obtained by pVA2198 was generated by PCR using the primer pair *ermF* left and *ermAM* right [35]. The erythromycin cassette was incorporated into the pGEM-T Easy vector, resulting in pGEM-T Easy-

ermF-ermAM. The pGEM-T Easy-*ermF-ermAM* plasmid was digested with *Sph*I and *Spe*I and the *ermF-ermAM* cassette was inserted into pPG0343UD, resulting in pPG0343UDErm (Table 1).

Transformation of *P. gingivalis*

P. gingivalis ΔPG0343 was constructed by allelic exchange via insertion of an erythromycin resistance determinant into *PG0343*. The plasmid pPG0343UDErm (Table 1) was prepared for disruption of *PG0343*. *PG0343*-deleted *P. gingivalis* strains containing pPG0343UDErm were obtained by electrotransformation (Table 1) according to Okamoto *et al*. [36].

H_2S and CH_3SH detection

Bacterial strains were cultured at 37°C to an OD at 600 nm (OD_{600}) of 0.6. Cultures were centrifuged, washed with phosphate-buffered saline (PBS) and resuspended in PBS to an OD_{600} of 0.3. The reaction mixture, which comprised 100 μL of cell suspension and 870 μL of PBS, was transferred to a 15-mL polypropylene tube with a silicon plug. The reaction was initiated by adding 30 μL of 33 mM L-cysteine or 33 mM L-methionine. The reaction mixtures were incubated at 37°C for 90 min, and the reaction was stopped by adding 500 μL of 3 M phosphoric acid. Ten minutes later, 1 mL of the vapor above the reaction mixture was analyzed by gas chromatography (Model GC-14B; Shimadzu Works, Tokyo, Japan) using a glass column packed with 25% b,b'-oxydipropionitrile on a 60–80 mesh Chromatosorb W AW-DMCS-ST (Shimadzu Works, Tokyo, Japan) fitted with a flame photometric detector at 70°C. Volatile sulfur compound (VSC) concentration was determined using standard H_2S, methyl mercaptan, or dimethyl sulfide gas prepared using a Permeater PD-1B (GL Science, Tokyo, Japan).

Preparation of recombinant enzyme and antisera

To produce recombinant *P. gingivalis* PG0343, PCR products generated using the PG0343SF-Nde or PG0343LF-Nde and PG0343R-Xho primers were inserted into pET16b (Novagen, Madison, WI) with

172 *Nde*I and *Xho*I sites to produce pET-16b-pg0343S (for PG0343 7–399) or pET-16b-pg0343L (for
173 PG0343 1–399), respectively (Fig. S1, Tables 1 and 2). The resulting plasmid was introduced into
174 *Escherichia coli* BL21 (TaKaRa, Tokyo, Japan). The transformant was cultured in 2× TY broth with
175 ampicillin (50 mg/mL) at 37°C to an OD_{600} of 0.8. Isopropyl-β-thiogalactopyranoside (IPTG) was
176 added to the culture to a final concentration of 1 mM, and the culture was incubated at 37°C for a
177 further 3 h. Cells were harvested by centrifugation and lysed by ultrasonication. Cell extract was
178 obtained by centrifugation of cell lysate. Recombinant proteins tagged with a histidine hexamer at the
179 N-terminus were purified using Ni^{2+}-nitrilotriacetic acid (NTA)-affinity chromatography as described
180 previously [37]. Anti-methionine-γ-lyase (PG0343) antibodies were prepared from a rabbit
181 immunized with *P. gingivalis* PG0343.

182 **Ethical statement**

183 All procedures for animal care were approved by the Animal Management Committee of Matsumoto
184 Dental University (Approval number: 275). All animal experiments were performed in compliance
185 with the Guidelines for Proper Conduct of Animal Experiments, established by Science Council of
186 Japan. Mice were housed in groups of four with 24 h access to food and water. The mice were
187 anesthetized with isoflurane and subjected to subcutaneous injections of 0.1 mL of bacterial
188 suspension at day 0. The lesion size and mortality were monitored eight hours interval each day.
189 The mice euthanasia were performed under isoflurane followed by cervical dislocation. If, the mice
190 were unable to move, they were immediately and humanely sacrificed by intraperitoneal injection of
191 sodium pentobarbital, then followed by cervical dislocation, and all efforts were made to minimize
192 suffering.

193 **Virulence assays**

194 *P. gingivalis* virulence was assayed as described previously [23, 24]. *P. gingivalis* W83 was cultured
195 in GAM broth supplemented with hemin and menadione to an OD_{600} of 1.0. The cells were harvested

and resuspended to 2.4×10^{10} or 2.4×10^{11} CFU/mL in PBS. To eliminate the effect of *P. gingivalis* LPS, Toll-like receptor (TLR)2 defective mice were used [38, 39]. BALB/c mice defective in TLR2 were purchased from Oriental Bio Science, Kyoto, Japan. BALB/c mice (female, 8 to 10 weeks old) and BALB/c TLR2$^{-/-}$ (female, 8 to 10 weeks old) were subjected to subcutaneous injections of 0.1 mL of bacterial suspension at two sites on the dorsal surface. After bacterial challenge, the extents of lesions were analyzed using ImageJ 1.38e software (National Institute of Health, Bethesda, MD; https://imagej.nih.gov/ij/).

Histological analysis

Two mice in each group were euthanized on day 5, when abscesses were evident. Tissues incorporating the whole abscess were dissected and fixed by perfusion with 4% paraformaldehyde in 0.05 M PBS. After dehydration, specimens were embedded in paraffin and sectioned serially. After deparaffinization, the sections were stained with hematoxylin and eosin, and visualized under a light microscope.

Statistical analysis

The Mann–Whitney U-test and one-way analysis of variance (ANOVA) were used to evaluate differences in lesion size between groups. The log-rank test was used to evaluate differences in survival rate. A value of $P < 0.05$ was considered to indicate statistical significance.

RESULTS

Identification of the H_2S-producing enzyme

To identify the *P. gingivalis* enzyme responsible for H_2S production from L-cysteine, we fractionated *P. gingivalis* proteins by gel filtration and performed activity staining (Fig. 1a and Fig. S1). The fractions exhibiting H_2S production (fraction number 46-49) were subjected to native PAGE and H_2S-production was visualized in the gel (Fig. 1b). The active band was excised and resolved by SDS-

PAGE. The gels were either stained with CBB R-250 or transferred to a PVDF membrane and stained with CBB R-250. The two prominent protein bands were NH_2-terminal sequenced directly on the membrane by Edman degradation (Fig. 1c). The resulting NH_2-terminal amino acid sequences (MKKEDLMR and MRSGFATR) were in agreement with the deduced amino acid sequence of PG0343, which has been identified as a methionine γ-lyase (Fig. S2ab).

Purification and characterization of PG0343

Recombinant PG0343 was purified and subjected to enzymatic analysis. SDS-PAGE indicated that the molecular weight of recombinant PG0343 was in agreement with the predicted value (44 kDa, Fig. 1d). Native PAGE and activity staining showed that recombinant PG0343 was associated with H_2S production from L-cysteine (Fig. 1e). In addition, the production of NH_3 and pyruvate, which are by-products of α, β–elimination of L-cysteine, was confirmed (data not shown). To evaluate the activity of recombinant PG0343, L-cysteine elimination was determined by monitoring pyruvate production. The K_m, $k_{cat,}$ and V_{max} values of PG0343 are shown in Table 3. The K_m values of PG0343 for L-cysteine and L-methionine were lower than those for *S*-methyl-L-cysteine and *S*-(2-aminoethyl)-L-cysteine, suggesting PG0343 to have affinity for L-cysteine and L-methionine as substrates.

Construction of PG0343 null mutant and Western blotting analysis

To evaluate its role in H_2S production, PG0343 was inactivated by allelic exchange mutagenesis. The resulting *P. gingivalis* ΔPG0343 was subjected to Western blotting, which confirmed the presence of PG0343 in *P. gingivalis* W83, but not ΔPG0343 (Fig. 2a).

Contribution of PG0343 to H_2S production by *P. gingivalis*

To confirm H_2S production by *P. gingivalis* Δ PG0343, we performed native PAGE and in-gel activity staining (Fig. 2b). H_2S production from L-cysteine by *P. gingivalis* ΔPG0343 was confirmed by activity staining. Gas chromatography showed that both *P. gingivalis* W83 and ΔPG0343 produced

242 H_2S from L-cysteine (Table 4 and Fig. 2b). These results indicate the presence of other enzymes that
243 catalyze production of H_2S from L-cysteine.

244 **Contribution of PG0343 to CH_3SH production by *P. gingivalis***

245 H_2S production by both *P. gingivalis* W83 and Δ PG0343 was increased circa 20-fold by adding L-
246 cysteine, while addition of L-cysteine or L-methionine did not affect CH_3SH production (Table 4). This
247 suggests that CH_3SH is produced constitutively by *P. gingivalis* W83, even in the absence of L-cysteine
248 and L-methionine.

249 **Effect of *P. gingivalis* on abscess formation**

250 To assess the role of *P. gingivalis* PG0343 in abdominal abscess formation in mice, the sizes of lesions
251 were analyzed after injection of *P. gingivalis* W83 and ΔPG0343 with or without L-cysteine into the
252 dorsum of mice. After 72 h, 6 of 10 and 4 of 10 mice injected with *P. gingivalis* with and without L-
253 cysteine, respectively, exhibited abdominal abscesses. *P. gingivalis* W83 formed larger abscesses than
254 *P. gingivalis* ΔPG0343 in the absence of L-cysteine (mean ± SD; 1.10 + 0.30 *vs.* 0.27 ± 0.24 cm^2, Fig.
255 3a; $P < 0.01$).

256 The survival rates of BALB/c mice injected with 4.8×10^{10} CFU/200 μL of *P. gingivalis*
257 W83 was 60% and 0% at 2 days and 3 days after injection, respectively, while no mouse died within
258 5 days of injection of the same number of *P. gingivalis* ΔPG0343 (Fig. 3b, $P < 0.001$). To eliminate
259 the effect of non-protein factors (*e.g.*, lipopolysaccharide [LPS]), we challenged BALB/c mice with
260 4.8×10^{10} CFU/200 μL of heat-killed or non-heat-killed *P. gingivalis* W83. After injection of non-
261 heat-killed *P. gingivalis* W83, 80% and 100% of the mice had died at day 2 and day 3, respectively,
262 while no mouse challenged with heat-killed *P. gingivalis* W83 died (Fig. 3c, $P < 0.001$). These results
263 suggest that heat-labile components of *P. gingivalis* W83 are involved in abscess formation.
264 Additionally, *P. gingivalis* W83 was injected into BALB/c mice and BALB/c mice defective in TLR2
265 ($TLR2^{-/-}$ mice). There was no significant difference in lesion size between BALB/c and $TLR2^{-/-}$ mice

(mean ± SD; 0.838 ± 0.34 *vs.* 0.770 ± 0.48 cm^2; Fig. 3d). Therefore, *P. gingivalis* W83 LPS is not involved in abscess formation.

Gas chromatography revealed that CH_3SH is constitutively produced by *P. gingivalis* W83 irrespective of the presence of L-cysteine and L-methionine. In contrast, H_2S production by *P. gingivalis* W83 was enhanced by adding L-cysteine (Table 4). Therefore, to analyze the role of H_2S produced by PG0343, abscess formation was analyzed in BALB/c mice challenged with *P. gingivalis* W83 with/without L-cysteine. At 12 h after injection, abdominal lesions were larger in mice challenged with *P. gingivalis* W83 supplemented with L-cysteine compared with *P. gingivalis* W83 only (mean ± SD; 0.84 ± 0.267 *vs.* 0.41 ± 0.087 cm^2, Fig. 4a; $P < 0.01$, n = 10 per group, one-way ANOVA). No abscess formation was observed in mice challenged with *P. gingivalis* ΔPG0343 supplemented with/without L-cysteine. After 72 h, lesions were larger in mice challenged with *P. gingivalis* W83 supplemented with than without L-cysteine (mean ± SD; 1.48 ± 0.38 *vs.* 0.41 ± 0.087 cm^2, Fig. 4B, $P < 0.05$; n = 10 per group, one-way ANOVA). *P. gingivalis* ΔPG0343 supplemented with/without L-cysteine formed smaller abscesses than did *P. gingivalis* W83 (Fig. 4b, $P < 0.01$, < 0.05, respectively; n = 10 per group, one-way ANOVA). In addition, there was no significant difference in abscess formation between *P. gingivalis* ΔPG0343 supplemented with and without L-cysteine (mean ± SD; 0.46 ± 0.28 *vs.* 0.27 ± 0.24 cm^2, Fig. 4b; n = 10 per group, one-way ANOVA). However, there was no significant difference in lesion size in *P. gingivalis* W83 and ΔPG0343 according to L-methionine supplementation (Fig. 4c, d; n = 10 per group, one-way ANOVA). Therefore, H_2S produced by PG0343 enhances CH_3SH-mediated abscess formation. However, H_2S produced by other enzymes seems to play a negligible role in abscess formation. Thus, production of both H_2S and CH_3SH by PG0343 enhances abscess formation relative to CH_3SH alone.

Histological analysis

Compared with mice challenged with *P. gingivalis* W83 without L-cysteine, a greater number of cells

infiltrated lesions in mice challenged with *P. gingivalis* W83 plus L-cysteine ($P < 0.05$; Fig. 5a, b).

DISCUSSION

Disruption of *mgl*, which encodes methionine-γ-lyase, in *P. gingivalis* abolishes abscess formation in mice [22, 23]. However, the mechanisms underlying abdominal abscess formation in mice by *P. gingivalis* had not been reported. Methionine-γ-lyase produces CH_3SH via L-methionine [40, 41]; therefore, we focused on the roles of other VSCs in abscess formation by *P. gingivalis.* We reported previously that *P. gingivalis* produces H_2S by degrading L-cysteine and/or DL-homocysteine [27]. H_2S reportedly exerts pro- and anti-inflammatory effects in different organisms. In this study, we identified an enzyme that catalyzes H_2S generation by degrading L-cysteine. The *P. gingivalis* protein fractions with H_2S-production activity were further analyzed to identify the protein responsible (PG0343), which was indistinguishable from methionine-γ-lyase.

We produced recombinant PG0343 and analyzed its H_2S production. Recombinant PG0343 produced H_2S by degrading L-cysteine; this activity has not been reported previously. To evaluate the role of PG0343 in H_2S production, we constructed a PG0343-deletion mutant (*P. gingivalis* ΔPG0343). Activity staining of *P. gingivalis* ΔPG0343 yielded a positive band. Gas chromatography, which is more sensitive than activity staining, verified production of H_2S by *P. gingivalis* ΔPG0343, which suggests the existence of other H_2S-producing enzymes.

P. gingivalis W83 produced CH_3SH constitutively, irrespective of the presence of L-methionine. However, H_2S production was enhanced by the addition of L-cysteine (31.74 ± 9.34 ng/mL), while H_2S production in the absence of L-cysteine was negligible (1.59 ± 0.28 ng/mL) (Table 4). Thus, CH_3SH production by *P. gingivalis* W83 is not dependent on L-methionine, while H_2S production is dependent on the presence of L-cysteine. Therefore, to assess the virulence of H_2S, mice were infected with *P. gingivalis* W83 strains supplemented with/without L-cysteine. Abdominal lesions produced by *P. gingivalis* W83 supplemented with L-cysteine were significantly larger than

314 those by *P. gingivalis* W83 without L-cysteine at 12 and 72 h after injection. However, there was no
315 significant difference in lesion size between *P. gingivalis* ΔPG0343 supplemented with and without L-
316 cysteine (Fig. 4a, b). In addition, the lesions produced by *P. gingivalis* ΔPG0343 were significantly
317 smaller than those by *P. gingivalis* W83, irrespective of the presence of L-cysteine (Fig. 4a, b).
318 Therefore, CH_3SH produced by PG0343 is essential for abscess formation in mice, and H_2S enhances
319 CH_3SH-induced abscess formation. These results indicate that abscess formation is induced by CH_3SH,
320 and that H_2S plays a supportive role in this process.

321 Ishihara *et al*. reported that *P. gingivalis* ATCC 33277 defective in gingipain (*rgpA*, *rgpB*,
322 and *kgp* triple mutant) formed few abscesses in BALB/cN mice [42]. In this study, we did not evaluate
323 the relationship between gingipain expression and PG0343; therefore, the possible role of PG0343 as
324 a regulator of gingipain genes should be clarified.

325 Furthermore, the role of *P. gingivalis* LPS for abscess formation was analyzed. There is
326 no significant differences in abscess formation by *P. gingivalis* W83 between BALB/c and $TLR2^{-/-}$
327 mice (Fig. 3d). These results indicated the *P. gingivalis* LPS is not a main source of mouse abscess
328 formation. Previous study reported that H_2S synergistically upregulated *P. gingivalis* LPS-induced
329 IL-6 and IL-8 expressions in fibroblasts and periodontal ligament cells via NF-κB signaling [43]. In
330 this study, we did not analyze the relationship between *P. gingivalis*-induced abscess formation and
331 activation of NF-κB signaling. To elucidate the mechanisms for abscess formation by *P. gingivalis*,
332 signaling pathway should be analyzed. This study should be useful for the development of inhibitor
333 for periodontal diseases.

334 Following subcutaneous injection into mice, *P. gingivalis*-generated H_2S did not induce
335 abscess formation, but accelerated abscess formation caused by CH_3SH. In this study, we did not
336 identify the mechanisms underlying this synergistic effect of CH_3SH and H_2S on abscess formation.
337 However, Stephen *et al*. reported that *P. gingivalis* W50 mutant, which lacks methionine-γ-lyase,

significantly alters the community composition of a 10-species biofilm co-culture model compared with the wild-type [44]. In addition, this mutant biofilm reduced IL-6, IL-8 and IL-1α production by keratinocytes compared with wild-type biofilm. Therefore, *P. gingivalis* methionine-γ-lyase affects microflora composition and proinflammatory cytokine production by keratinocytes and enhances the inflammatory response. H_2S accelerates the inflammatory response induced by methionine-γ-lyase. *P. gingivalis* methionine-γ-lyase also affects biofilm composition; therefore, the role of H_2S in biofilm formation induced by methionine-γ-lyase should be determined.

In conclusion, we identified an enzyme that catalyzes the generation of H_2S from L-cysteine in *P. gingivalis* W83 as a methionine-γ-lyase (PG0343). H_2S produced by degradation of L-cysteine enhanced abscess formation by CH_3SH, but H_2S itself did not affect abscess formation. The mechanisms underlying this synergistic effect of methyl mercaptan and H_2S on oral inflammation and microbiota composition should be elucidated.

Figure Legends

Fig. 1. Isolation of a hydrogen sulfide (H_2S) –producing enzyme from *P. gingivalis* W83. (a) Protein fractions with H_2S production are indicated (arrow). (b) Fraction Nos. 1 and 2 were resolved by native polyacrylamide gel electrophoresis (PAGE) and subjected to activity staining. (c) Positive bands were resolved by sodium dodecyl sulfate (SDS)-PAGE, transferred to a polyvinylidene difluoride (PVDF) membrane, and stained with Coomassie Brilliant Blue (CBB) R-250. The two bands indicated by arrows were subjected to NH_2-terminal amino acid sequencing. (d) Purification of recombinant PG0343. Lane M, size marker; lane 1, *E. coli* BL21 + pET-16b; lane 2, *E. coli* BL21 + pET-16b-pg0343L; lane 3, *E. coli* BL21 + pET-16b-pg0343L + IPTG (+); lane 4, purified protein. (e) Native PAGE and activity staining of recombinant PG0343L (lane 1) and recombinant PG0343S (lane 2).

Fig. 2. Characterization of the *P. gingivalis* PG0343-deletion mutant. (a) Immunoblot analysis of

PG0343 using anti-PG0343 antiserum. Lane 1, *P. gingivalis* W83, lane 2, *P. gingivalis* PG0343-deletion mutant. (b) Activity staining of *P. gingivalis* whole-cell lysate. Lane 1, *P. gingivalis* W83, lane 2, *P. gingivalis* PG0343-deletion mutant.

Fig. 3. Virulence assay of *P. gingivalis*. (a) Lesion size of BALB/c mice challenged with *P. gingivalis* W83 or the *P. gingivalis* PG0343-deletion mutant (72 h, $P < 0.01$, Mann–Whitney U-test, n = 10). (b) Survival rates of mice challenged with *P. gingivalis* W83 or the *P. gingivalis* PG0343-deletion mutant ($P < 0.01$, log-rank test, n = 5 per group). (c) Survival rates of mice challenged with untreated or heat-killed *P. gingivalis* W83 ($P < 0.01$, log-rank test, n = 5 per group). (d) Lesion size of BALB/c and BALB/c TLR2$^{-/-}$ mice challenged with *P. gingivalis* W83 (72 h, $P < 0.01$, Mann–Whitney U-test, n = 4 for BALB/c mice and n = 3 for BALB/c TLR2$^{-/-}$ mice).

Fig. 4. Lesion size of mice challenged with *P. gingivalis* supplemented with/without L-cysteine or DL-methionine. (ab) *P. gingivalis* supplemented with/without L-cysteine (a 12 h and b 72 h after injection, n = 10 per group). (cd) *P. gingivalis* supplemented with/without DL-methionine (c 12 h and d 72 h after injection, n = 10 per group). *, $P < 0.05$; **, $P < 0.05$; NS, not significant.

Fig. 5. Histological analysis of subcutaneous abdominal lesions. Subcutaneous lesion challenged with/without *P. gingivalis* W83 supplemented with/without 10 mM L-cysteine (72 h).

Supporting Information

Fig. S1. Fractionation of *Porphyromonas gingivalis* W83 lysates by gel filtration. The bar indicates active fractions (fraction number 46 to 49).

Fig. S2. Amino acid sequence and starting position of two ORFs of PG0343. (a) Two ORFs of PG0343. (b) Amino acid sequence of PG0343.

Funding information

This work was supported in parts by a Grant-in-Aid for Scientific Research (B) (Grant Number 15H05297) to A.Y. and by Grant-in-Aid for Challenging Exploratory Research (Grant Number 26560405) to B.Y.H. from the Japan Society for the Promotion of Science (JSPS).

Conflicts of interest

The authors declare that there are no conflicts of interest.

References

1. **Lo Faro ML, Fox B, Whatmore JL, Winyard PG, Whiteman M.** Hydrogen sulfide and nitric oxide interactions in inflammation. *Nitric Oxide* 2014; 41:38-47.

2. **Kimura H.** Hydrogen Sulfide and Polysulfide Signaling. *Antioxid Redox Signal* 2017; 27: 619-621.

3. **Bianco CL, Fukuto JM.** Examining the reaction of NO and H_2S and the possible cross-talk between the two signaling pathways. *Proc Natl Acad Sci U S A* 2015;112:10573-10574.

4. **Liu Y, Yang R, Liu X, Zhou Y, Qu C, Kikuiri T, Wang S, Zandi E, Du J, Ambudkar IS, Shi S.** Hydrogen sulfide maintains mesenchymal stem cell function and bone homeostasis via regulation of Ca^{2+} channel sulfhydration. *Cell Stem Cell* 2014;15:66-78.

5. **Lloyd D.** Hydrogen sulfide: clandestine microbial messenger? *Trends Microbiol* 2006;14:456-462.

6. **Kabil O, Motl N, Banerjee R.** H_2S and its role in redox signaling. *Biochim Biophys Acta* 2014;1844:1355-1366.

7. **Shatalin K, Shatalina E, Mironov A, Nudler E.** H_2S: a universal defense against antibiotics in bacteria. *Science* 2011; 334:986-990.

8. **Kimura Y, Goto Y, Kimura H.** Hydrogen sulfide increases glutathione production and suppresses oxidative stress in mitochondria. *Antioxid Redox Signal* 2010;12:1-13.

9. **Sun WH, Liu F, Chen Y, Zhu YC.** Hydrogen sulfide decreases the levels of ROS by inhibiting mitochondrial complex IV and increasing SOD activities in cardiomyocytes under ischemia/reperfusion. *Biochem Biophys Res Commun* 2012;421:164-169.

10. **Manna P, Jain SK.** L-cysteine and hydrogen sulfide increase PIP3 and AMPK/PPARγ expression and decrease ROS and vascular inflammation markers in high glucose treated human U937 monocytes. *J Cell Biochem* 2013; 114:2334-2345.

11. **Kassem A, Henning P, Lundberg P, Souza PP, Lindholm C, Lerner UH.** *Porphyromonas gingivalis* Stimulates Bone Resorption by Enhancing RANKL (Receptor Activator of NF-κB Ligand) through Activation of Toll-like Receptor 2 in Osteoblasts. *J Biol Chem* 2015; 290:20147-20158.

12. **Malcolm J, Awang RA, Oliver-Bell J, Butcher JP, Campbell L, Adrados Planell A, Lappin DF, Fukada SY, Nile CJ, Liew FY, Culshaw S.** IL-33 Exacerbates Periodontal Disease through Induction of RANKL. *J Dent Res* 2015; 94:968-75.

13. **Malcolm J, Millington O, Millhouse E, Campbell L, Adrados Planell A, Butcher JP, Lawrence C, Ross K, Ramage G, McInnes IB, Culshaw S.** Mast Cells Contribute to *Porphyromonas gingivalis*-induced Bone Loss. *J Dent Res* 2016;95:704-710.

14. **Prates TP, Taira TM, Holanda MC, Bignardi LA, Salvador SL, Zamboni DS, Cunha FQ, Fukada SY.** NOD2 contributes to *Porphyromonas gingivalis*-induced bone resorption. *J Dent Res* 2014; 93:1155-1162.

15. **Han YW, Wang X.** Mobile microbiome: oral bacteria in extra-oral infections and inflammation. *J Dent Res* 2013; 92:485-491.

16. **Hajishengallis G, Liang S, Payne MA, Hashim A, Jotwani R, Eskan MA, McIntosh ML, Alsam A, Kirkwood KL, Lambris JD, Darveau RP, Curtis MA.** Low-abundance biofilm

species orchestrates inflammatory periodontal disease through the commensal microbiota and complement. *Cell Host Microbe* 2011;10:497-506.

17. **Darveau RP, Hajishengallis G, Curtis MA.** *Porphyromonas gingivalis* as a potential community activist for disease. *J Dent Res* 2012;91:816-820.

18. **Hajishengallis G, Darveau RP, Curtis MA.** The keystone-pathogen hypothesis. *Nat Rev Microbiol* 2012;10:717-725.

19. **Fitzgerald JR, Foster TJ, Cox D.** The interaction of bacterial pathogens with platelets. *Nat Rev Microbiol* 2006;4:445-457.

20. **Radwan-Oczko M, Jaworski A, Duś I, Plonek T, Szulc M, Kustrzycki W.** *Porphyromonas gingivalis* in periodontal pockets and heart valves. *Virulence* 2014;5:575-80.

21. **Velsko IM, Chukkapalli SS, Rivera MF, Lee JY, Chen H, Zheng D, Bhattacharyya I, Gangula PR, Lucas AR, Kesavalu L.** Active invasion of oral and aortic tissues by *Porphyromonas gingivalis* in mice causally links periodontitis and atherosclerosis. *PLoS One* 2014;9:e97811.

22. **Slocum C, Coats SR, Hua N, Kramer C, Papadopoulos G, Weinberg EO, Gudino CV, Hamilton JA, Darveau RP, Genco CA.** Distinct lipid a moieties contribute to pathogen-induced site-specific vascular inflammation. *PLoS Pathog* 2014;10:e1004215.

23. **Widziolek M, Prajsnar TK, Tazzyman S, Stafford GP, Potempa J, Murdoch C.** Zebrafish as a new model to study effects of periodontal pathogens on cardiovascular diseases. *Sci Rep* 2016;6:36023.

24. **Persson S, Claesson R, Carlsson J.** The capacity of subgingival microbiotas to produce volatile sulfur compounds in human serum. *Oral Microbiol Immunol* 1989; 4:169-172.

451 25. **Persson S, Edlund M-B, Claesson R, Carlsson J.** The formation of hydrogen sulfide and
452 methyl mercaptan by oral bacteria. *Oral Microbiol Immunol* 1990;5:195-201.

453 26. **Yoshimura M, Nakano Y, Yamashita Y, Oho T, Saito T, Koga T.** Formation of methyl
454 mercaptan from L-methionine by *Porphyromonas gingivalis*. *Infect Immun* 2000;68:6912-6.

455 27. **Yoshimura M, Nakano Y, Koga T.** L-Methionine-gamma-lyase, as a target to inhibit
456 malodorous bacterial growth by trifluoromethionine. *Biochem Biophys Res Commun*
457 2002;292:964-968.

458 28. **Ng W, Tonzetich J.** Effect of hydrogen sulfide and methyl mercaptan on the permeability of
459 oral mucosa. *J Dent Res* 1984;63:994–997.

460 29. **Ratkay LG, Waterfield JD, Tonzetich J.** Stimulation of enzyme and cytokine production by
461 methyl mercaptan in human gingival fibroblast and monocyte cell cultures. *Arch Oral Biol*
462 1995;40:337-344.

463 30. **Nakano Y, Yoshimura M, Koga T.** Methyl mercaptan production by periodontal bacteria.
464 *Int Dent J* 2002; Suppl 3: 217-220.

465 31. **Yoshida A, Yoshimura M, Ohara N, Yoshimura S, Nagashima S, Takehara T, Nakayama K.**
466 Hydrogen sulfide production from cysteine and homocysteine by periodontal and oral bacteria. *J*
467 *Periodontol* 2009; 80:1845-1851.

468 32. **Chen W, Kajiya M, Giro G, Ouhara K, Mackler HE, Mawardi H, Boisvert H, Duncan MJ,**
469 **Sato K, Kawai T.** Bacteria-derived hydrogen sulfide promotes IL-8 production from epithelial
470 cells. *Biochem Biophys Res Commun* 2010;391:645-650.

471 33. **Yoshida Y, Suwabe K, Nagano K, Kezuka Y, Kato H, Yoshimura F.** Identification and
472 enzymic analysis of a novel protein associated with production of hydrogen sulfide and L-serine

from L-cysteine in *Fusobacterium nucleatum* subsp. nucleatum ATCC 25586. *Microbiology* 2011;157:2164-2171.

34. **Yoshimura M, Nakano Y, Fukamachi H, Koga T.** 3-Chloro-DL-alanine resistance by L-methionine-alpha-deamino-gamma-mercaptomethane-lyase activity. *FEBS Lett* 2002;523:119-122.

35. **Fletcher HM, Schenkein HA, Morgan RM, Bailey KA, Berry CR, Macrina FL.** Virulence of a *Porphyromonas gingivalis* W83 mutant defective in the *prtH* gene. *Infect Immun* 1995;63:1521-1528.

36. **Okamoto K, Nakayama K, Kadowaki T, Abe N, Ratnayake DB, Yamamoto K.** Involvement of a lysine-specific cysteine proteinase in hemoglobin adsorption and heme accumulation by *Porphyromonas gingivalis*. *J Biol Chem* 1998;273:21225-21231.

37. **Singh KV, La Rosa SL, Singh KV, Somarajan SR, Roh JH, Murray BE.** The fibronection-binding protein EfbA contributes to pathogenesis and protects against infective endocarditis caused by *Enterococcus faecalis*. *Infect Immun* 2015;83:4487-4494.

38. **Tang X, Metzger D, Leeman S, Amar S.** LPS-induced TNF-alpha factor (LITAF)-deficient mice express reduced LPS-induced cytokine: Evidence for LITAF-dependent LPS signaling pathways. *Proc Natl Acad Sci U S A* 2006;103:13777-13782.

39. **Hajishengallis G, Tapping RI, Harokopakis E, Nishiyama S, Ratti P, Schifferle RE, Lyle EA, Triantafilou M, Triantafilou K, Yoshimura F.** Differential interactions of fimbriae and lipopolysaccharide from *Porphyromonas gingivalis* with the Toll-like receptor 2-centred pattern recognition apparatus. *Cell Microbiol* 2006;8:1557-1570.

40. **Faleev NG, Alferov KV, Tsvetikova MA, Morozova EA, Revtovich SV, Khurs EN, Vorob'ev MM, Phillips RS, Demidkina TV, Khomutov RM.** Methionine gamma-lyase: mechanistic

deductions from the kinetic pH-effects. The role of the ionic state of a substrate in the enzymatic activity. *Biochim Biophys Acta* 2009;1794:1414-1420.

41. **Hanniffy SB, Philo M, Peláez C, Gasson MJ, Requena T, Martínez-Cuesta MC.** Heterologous production of methionine-gamma-lyase from *Brevibacterium linens* in *Lactococcus lactis* and formation of volatile sulfur compounds. *Appl Environ Microbiol* 2009;75:2326-2332.

42. **Ishihara Y, Anan H, Yoneda M, Maeda K, Hirofuji T.** Susceptibility of type 2 diabetic mice to low-virulence bacterial infection: induction of abscess formation by gingipain-deficient *Porphyromonas gingivalis*. *J Periodontal Res* 2007;42:253-258.

43. **Chi XP, Ouyang XY, Wang YX.** Hydrogen sulfide synergistically upregulates Porphyromonas gingivalis lipopolysaccharide-induced expression of IL-6 and IL-9 via NF-κB signaling in periodontal fibroblasts. *Arch Oral Biol* 2014: 59: 954-961.

44. **Stephen AS, Millhouse E, Sherry L, Aduse-Opoku J, Culshaw S, Ramage G, Bradshaw DJ, Burnett GR, Allaker RP.** In Vitro Effect of *Porphyromonas gingivalis* Methionine Gamma Lyase on Biofilm Composition and Oral Inflammatory Response. *PLoS One* 2016;11:e0169157.

The English in this document has been checked by at least two professional editors, both native speakers of English. For a certificate, please see:

http://www.textcheck.com/certificate/rY9Ov4

518 Table 1. Strains and plasmids used in this study

Strains or plasmid	Description	Source or reference
Strains		
Porphyromonas gingivalis W83	Oral commensal	RIKEN*
Escherichia coli DH5α	Cloning host	TaKaRa
Escherichia coli BL21	Protein expression	TaKaRa
Plasmids		
pET-16b	Amp^r†, expression vector	Novagen
pET-16b-pg0343L	Production of His_{10}-PG0343(1-399)	This study
pET-16b-pg0343S	Production of His_{10}-PG0343(7-399)	This study
pGEM-T Easy	Amp^r, TA cloning	Promega
pGEM-T Easy-*ermF*-*ermAM*	Erm^r‡, contains the *ermF-ermAM* cassette in pGEM-T Easy	This study
pBluescript $SKII^+$	Amp^r, cloning vector	Stratagene
pPG0343UD	pBluescript $SKII^+$ harboring the upstream and downstream regions of PG0343	This study
pPG0343UDErm	pBluescript $SKII^+$ harboring the upstream and downstream regions of PG0343 and *ermF* cassette between upstream and downstream fragments	This study
pVA2198	*ermF-ermAM* cassette	[35]

519 *RIKEN BioResource Center, Wako, Japan

520 †Amp^r, ampicillin-resistant

521 ‡Erm^r, erythromycin-resistant

522

523 Table 2. Primers used in this study

Primer	Sequence* (5'→3')	Gene targeted
PG0343UF-Apa	ATGCGAGGGCCCCCACGGATTTCTATTGGGAAG	PG0343 upstream
PG0343UR-Sph	CTACATGCATGCAATCGAAGAATCGACGACCG	PG0343 upstream
PG0343DF-Spe	GTAGCAACTAGTAGGCTGCATAAAGGCCTGAC	PG0343 downstream
PG0343DR-Sac	TCGCTAGAGCTCTCGAATGTGCTACCGTTGGATC	PG0343 downstream
PG0343SF-Nde	GGAATTCCATATGCGTAGTGGCTTTGCCAC	PG0343S expression
PG0343LF-Nde	GGAATTCCATATGAAAAAAGAAGACCTTATGCG	PG0343L expression
PG0343R-Xho	TGCCGCTCGAGTTAGATCAGGCTGTCCAGACC	PG0343S/L expression
ermF left	CCGATAGCTTCCGCTATTGC	*ermF-ermAM* cassette
ermAM right	GGTATACTACTGACAGCTTC	*ermF-ermAM* cassette

524 *Endonuclease restriction sites are underlined.

525

526

527 Table 3. Kinetic properties of the PG0343*

Substrate	K_m (mM)	k_{cat} (sec^{-1})	k_{cat}/K_m ($sec^{-1}mM^{-1}$)	V_{max} (μmol/min/mg)
L-cysteine	1.03 ± 0.21	0.24 ± 0.03	0.234 ± 0.018	0.223 ± 0.029
L-methionine	1.88 ± 0.43	0.25 ± 0.11	0.128 ± 0.042	0.157 ± 0.023
S-methyl-L-cysteine	3.56 ± 1.22	0.53 ± 0.21	0.146 ± 0.018	0.422 ± 0.209
S-(2-aminoethyl) -L-cysteine	38.0 ± 10.0	0.10 ± 0.03	0.003 ± 0.001	0.105 ± 0.035

528 *mean ± S.D. (n=4)

529

530

Table 4. Hydrogen sulfide and methyl mercaptan production by *P. gingivalis**

	H_2S (ng/mL)		CH_3SH (ng/mL)		VSCs (ng/mL)	
	W83	Δ PG0343	W83	Δ PG0343	W83	Δ PG0343
Base	1.59 ± 0.28	0.92 ± 0.20	71.6 ± 8.51	2.42 ± 0.20	73.2 ± 8.78	3.34 ± 0.25
+ L-cysteine	31.7 ± 9.34	28.2 ± 10.6	70.3 ± 6.81	4.68 ± 1.00	102 ± 13.5	32.9 ± 11.5
+ L-methionine	1.46 ± 0.22	0.73 ± 0.33	78.3 ± 3.13	2.27 ± 0.57	79.7 ± 3.21	3.00 ± 0.89

*mean ± S.D. (n=3)

Figure 1

Click here to download Figure Fig. 1.tiff

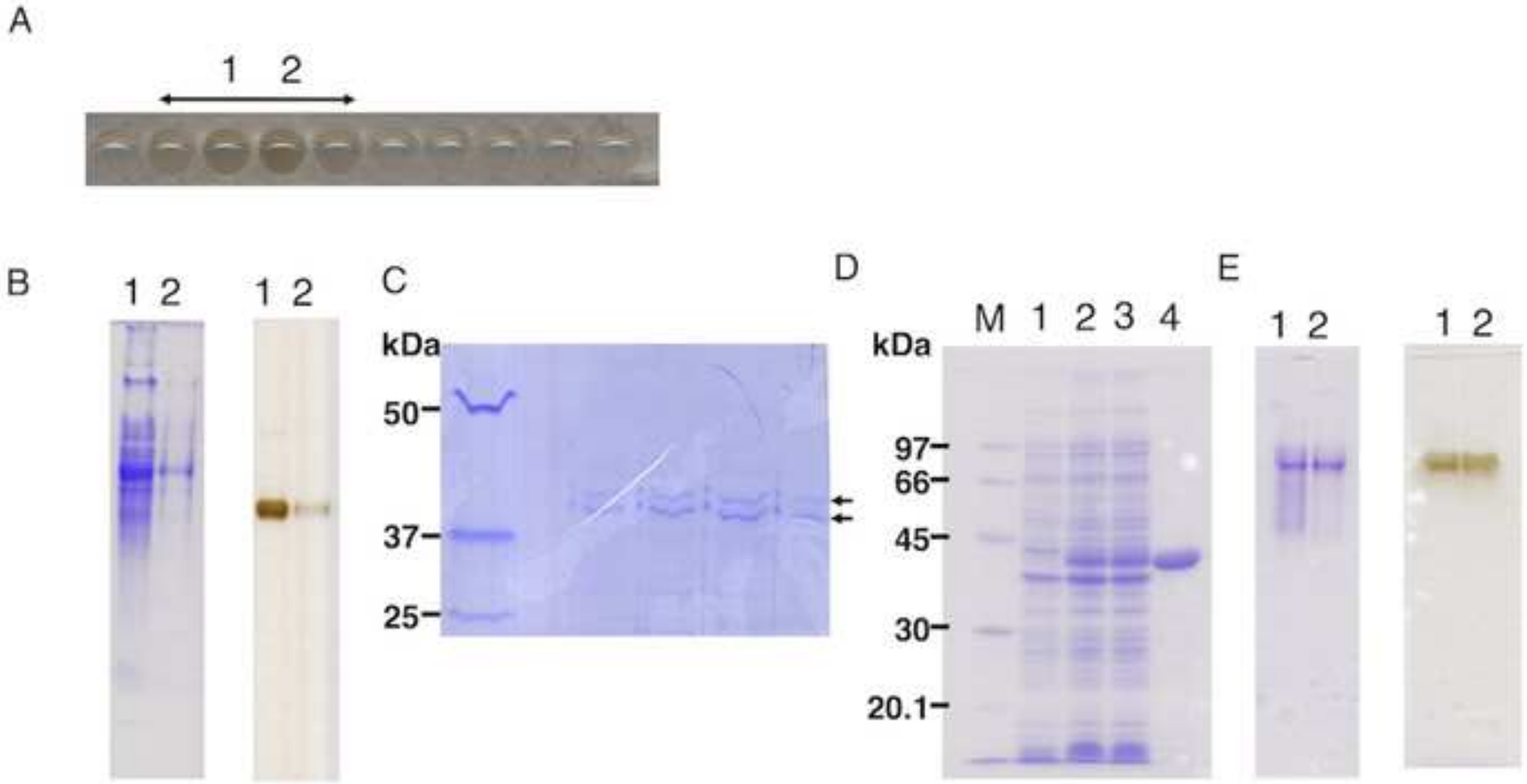

Figure 2

Click here to download Figure Fig. 2.tiff

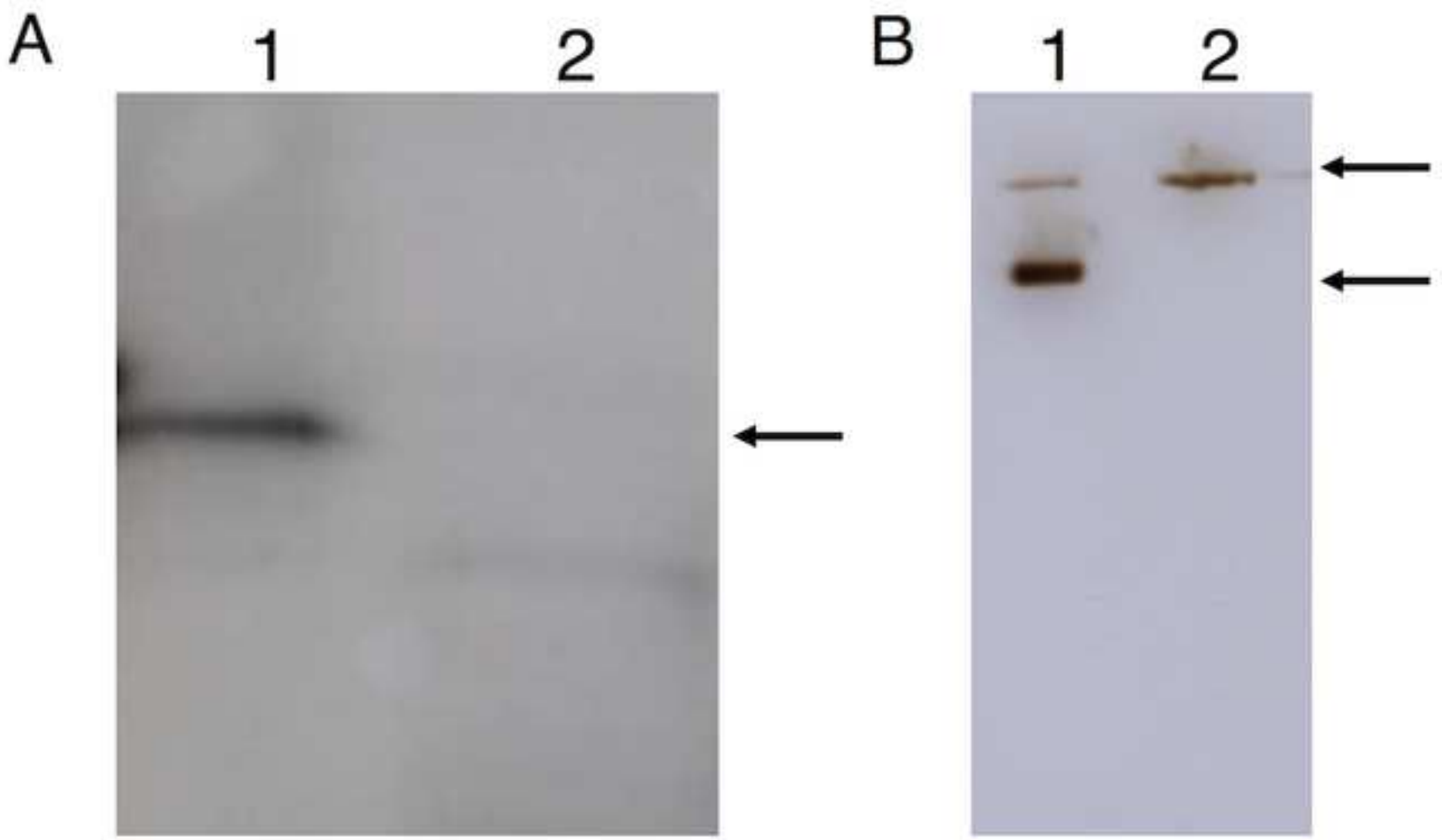

Figure 3

Click here to download Figure Fig. 3.tiff

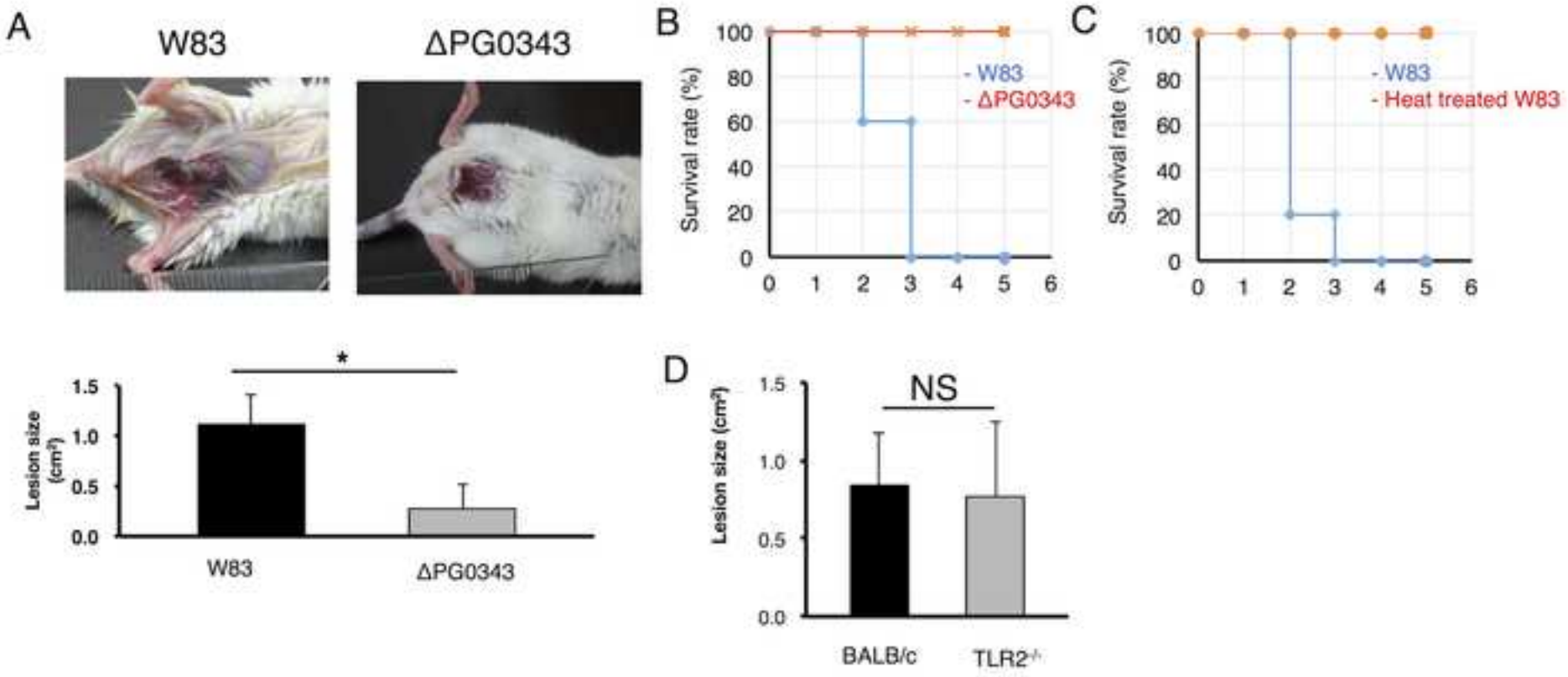

Figure 4

Click here to download Figure Fig. 4.tiff

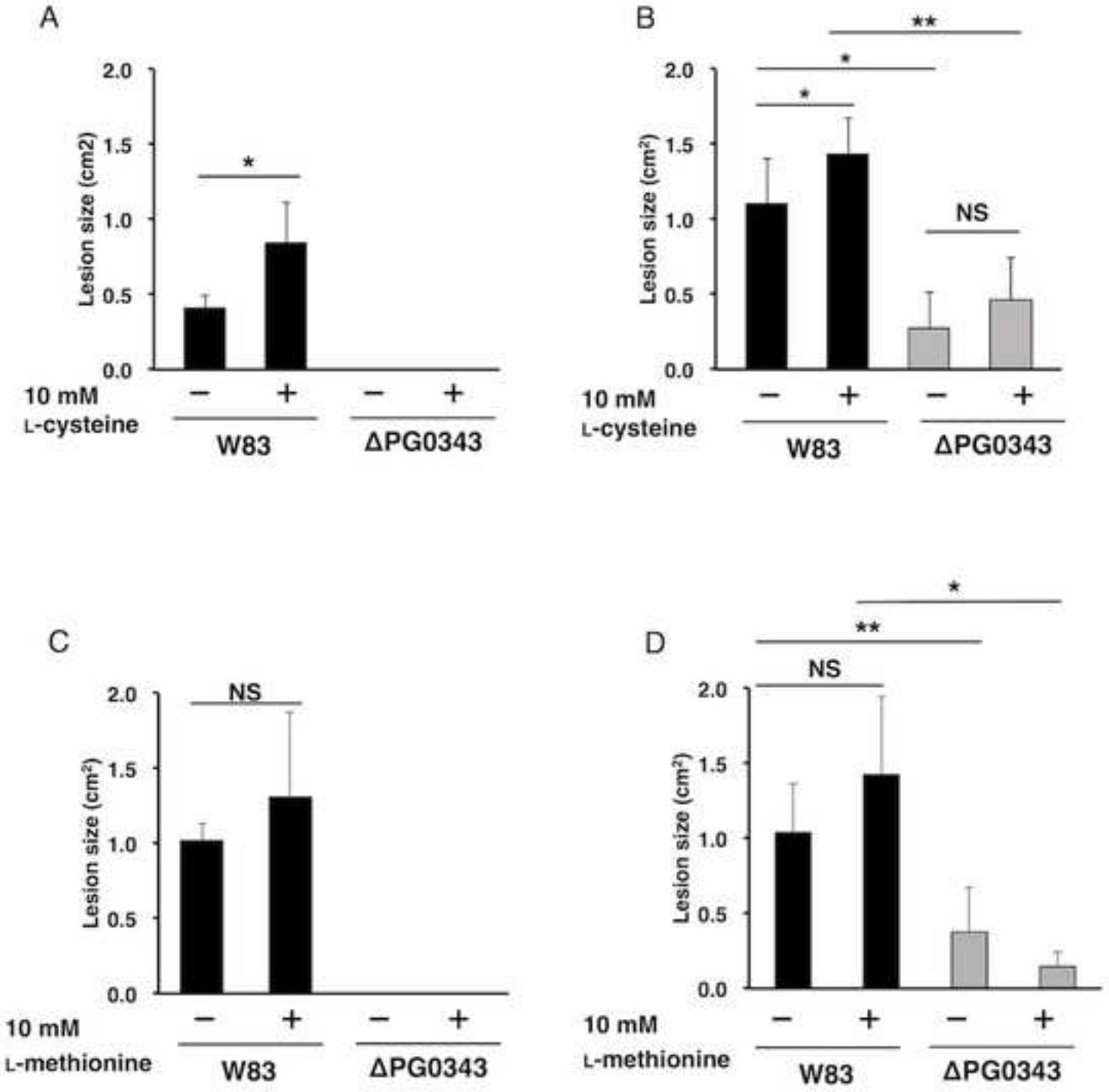

Figure 5

Click here to download Figure Fig. 5.tiff

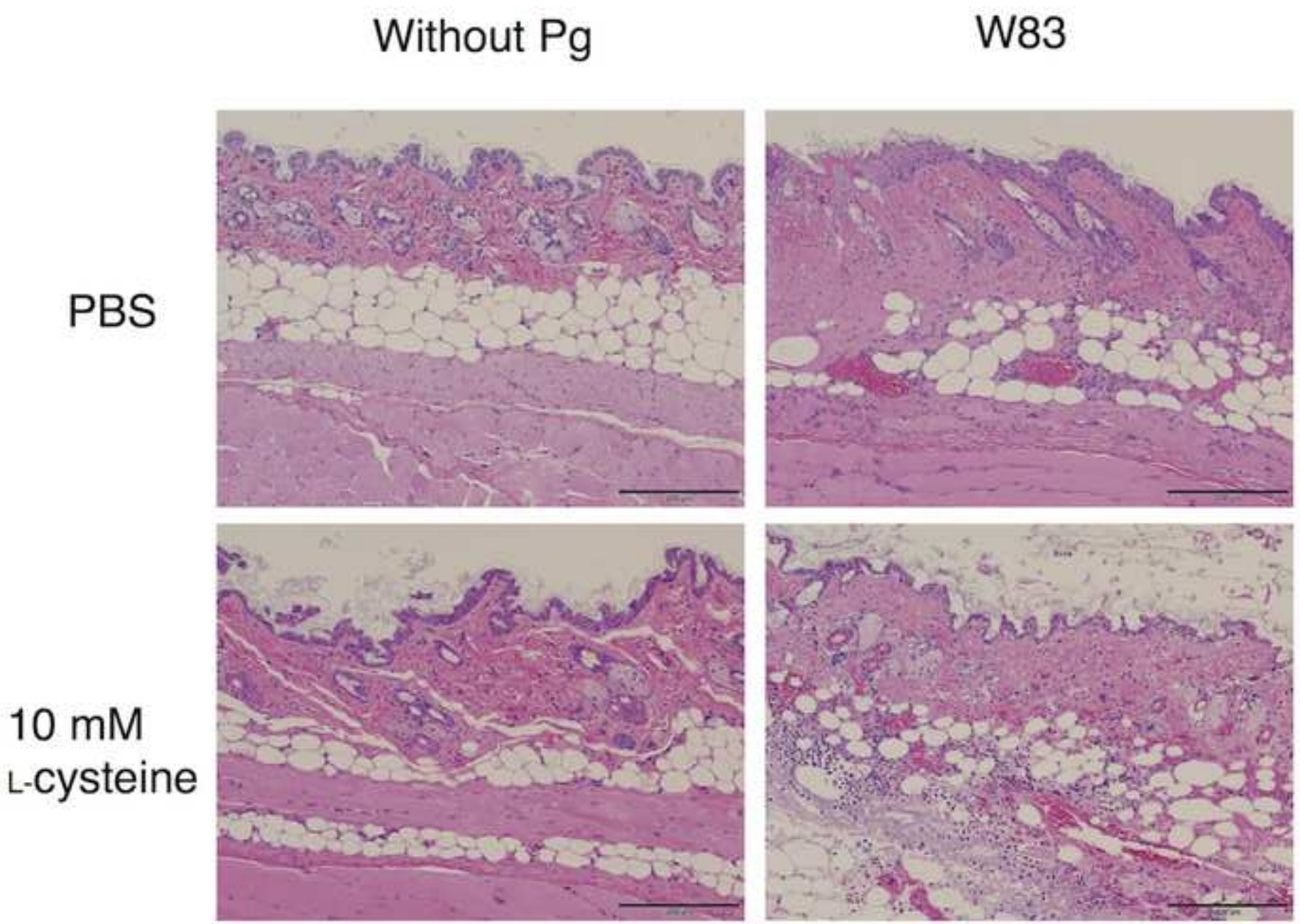

Click here to access/download
Response to Reviewer
R2R.doc

Supplementary Material Files

Click here to download Supplementary Material Files Nakamura H2S Suppl.Figs. 180127.pdf

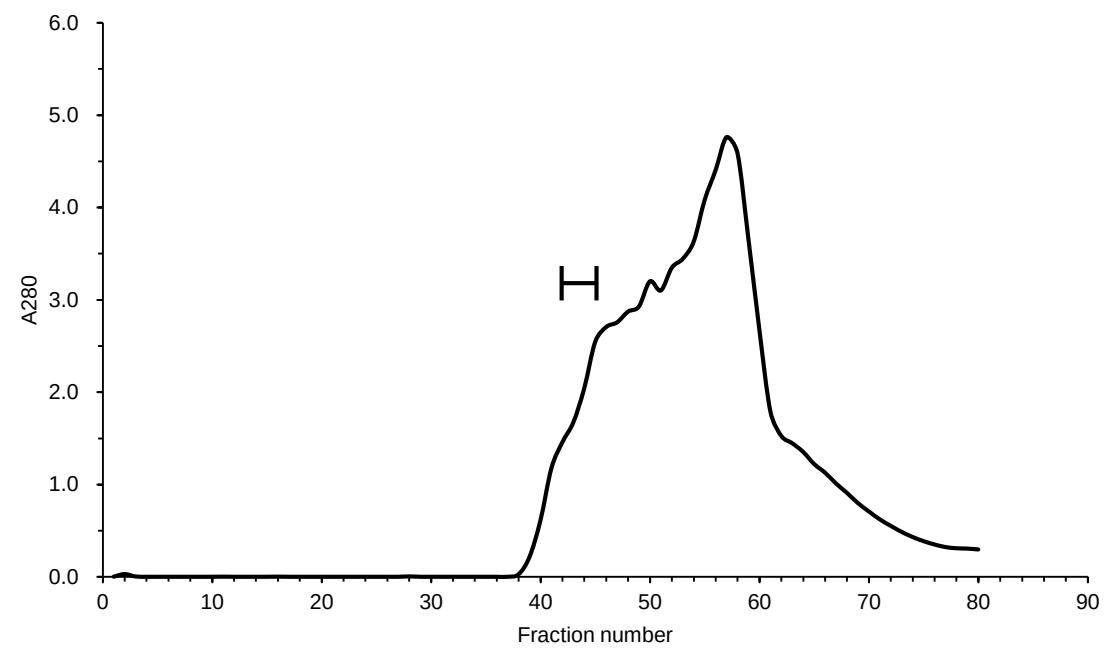

S1 Fig. Fractionation of *Porphyromonas gingivalis* W83 lysates by gel filtration. The bar indicates active fractions (fraction number 46 to 49).

A

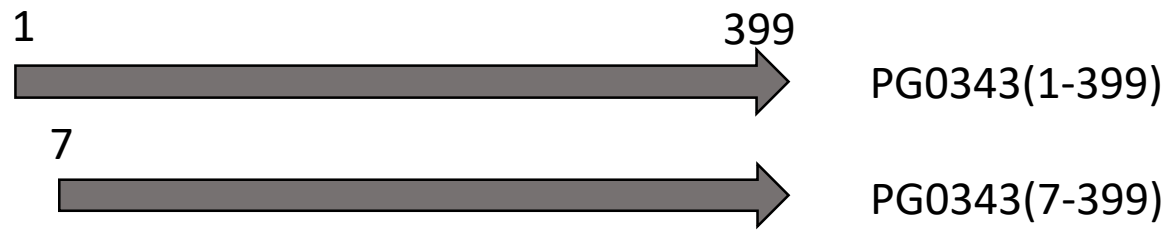

B

```
    *       *
  1 MKKEDLMRSG FATRAIHGGA IENAFGCLAT PIYQTSTFVF DTAEQGGRRF AGEEDGYIYT  60
 61 RLGNPNCTQV EEKLAMLEGG EAAASASSGI GAISSAIWVC VKAGDHIVAG KTLYGCTFAF 120
121 LTHGLSRYGV EVTLVDTRHP EEVEAAIRPN TKLVYLETPA NPNMYLTDIK AVCDIAHKHE 180
181 GVRVMVDNTY CTPYICRPLE LGADIVVHSA TKYLNGHGDV IAGFVVGKED YIKEVKLVGV 240
241 KDLTGANMSP FDAYLISRGM KTLQIRMEQH CRNAQTVAEF LEKHPAVEAV YFPGLPSFPQ 300
301 YELAKKQMAL PGAMIAFEVK GGCEAGKKLM NNLHLCSLAV SLGDTETLIQ HPASMTHSPY 360
361 TPEERAASDI SEGLVRLSVG LENVEDIIAD LKHGLDSLI
```

S2 Fig. Amino acid sequence and starting position of two ORFs of PG0343. **A.** Two ORFs of PG0343.
B. Amino acid sequence of PG0343.